JCI The Journal of Clinical Investigation

Myocardial infarction triggers cardioprotective antigen-specific T helper cell responses

Max Rieckmann, … , Ulrich Hofmann, Gustavo Campos Ramos

J Clin Invest. 2019. https://doi.org/10.1172/JCI123859.

Research In-Press Preview Cardiology Immunology

T cell autoreactivity is a hallmark of autoimmune diseases but can also benefit self-maintenance and foster tissue repair. Herein, we investigated whether heart-specific T cells exert salutary or detrimental effects in the context of myocardial infarction (MI), the leading cause of death worldwide. After screening more than 150 class-II-restricted epitopes, we found that myosin heavy chain alpha (MYHCA) was a dominant cardiac antigen triggering post-MI $CD4^+$ T cell activation in mice. Transferred MYHCA614-629-specific $CD4^+$ T (TCR-M) cells selectively accumulated in the myocardium and mediastinal lymph nodes (med-LN) of infarcted mice, acquired a Treg phenotype with a distinct pro-healing gene expression profile, and mediated cardioprotection. Myocardial Treg cells were also detected in autopsies from patients who suffered a MI. Noninvasive PET/CT imaging using a CXCR4 radioligand revealed enlarged med-LNs with increased cellularity in MI-patients. Notably, the med-LN alterations observed in MI patients correlated with the infarct size and cardiac function. Taken together, the results obtained in our study provide evidence showing that MI-context induces pro-healing T cell autoimmunity in mice and confirms the existence of an analogous heart/med-LN/T cell axis in MI patients.

Myocardial infarction triggers cardioprotective antigen-specific T helper cell responses

Authors: Max Rieckmann[1], Murilo Delgobo[2,3], Chiara Gaal[2,3], Lotte Büchner[2,3], Philipp Steinau[1], Dan Reshef[4], Cristina Gil-Cruz[5], Ellis N. ter Horst[6-9], Malte Kircher[10], Theresa Reiter[2], Katrin G. Heinze[11], Hans W. M. Niessen[7, 8], Paul A. J. Krijnen[7, 8], Anja M. van der Laan[6], Jan J. Piek[6, 8], Charlotte Koch[1], Hans-Jürgen Wester[12], Constantin Lapa[10], Wolfgang R. Bauer[2], Burkhard Ludewig[5], Nir Friedman[4], Stefan Frantz[1, 2, 3†], Ulrich Hofmann[1, 2, 3†], Gustavo Campos Ramos[1, 2, 3†*]

Affiliations:

[1] Department of Internal Medicine III, University Clinic Halle, Halle, Germany

[2] Department of Internal Medicine I, University Hospital Wuerzburg, Wuerzburg, Germany

[3] Comprehensive Heart Failure Center, University Hospital Wuerzburg, Wuerzburg, Germany

[4] Department of Immunology, Weizmann Institute of Science, Rehovot, Israel

[5] Institute of Immunobiology, Kantonsspital St. Gallen, St. Gallen, Switzerland

[6] Heart Center, Amsterdam UMC, location AMC, Amsterdam, the Netherlands

[7] Department of Pathology and Cardiac Surgery, Amsterdam UMC, location VUmc, Amsterdam, the Netherlands.

[8] Amsterdam Cardiovascular Sciences, Amsterdam UMC, Amsterdam, the Netherlands

[9] Netherlands Heart Institute, Utrecht, the Netherlands

[10] Department of Nuclear Medicine, University Hospital Wuerzburg, Wuerzburg, Germany

[11] Rudolf Virchow Center for Experimental Biomedicine, University of Wuerzburg, Wuerzburg, Germany

[12] Pharmaceutical Radiochemistry, Technical University Munich, Munich, Germany

[†] Shared last authorship

***Corresponding author:**

Dr. Gustavo Ramos
Immunocardiology Lab

Am Schwarzenberg 15, Haus A15
D-97078 Würzburg
Phone: +49 931 – 201 46477
Fax: +49 931 – 201 46485
E-mail:ramos_g@ukw.de

Abstract:

T cell autoreactivity is a hallmark of autoimmune diseases but can also benefit self-maintenance and foster tissue repair. Herein, we investigated whether heart-specific T cells exert salutary or detrimental effects in the context of myocardial infarction (MI), the leading cause of death worldwide. After screening more than 150 class-II-restricted epitopes, we found that myosin heavy chain alpha (MYHCA) was a dominant cardiac antigen triggering post-MI $CD4^+$ T cell activation in mice. Transferred $MYHCA_{614-629}$-specific $CD4^+$ T (TCR-M) cells selectively accumulated in the myocardium and mediastinal lymph nodes (med-LN) of infarcted mice, acquired a Treg phenotype with a distinct pro-healing gene expression profile, and mediated cardioprotection. Myocardial Treg cells were also detected in autopsies from patients who suffered a MI. Noninvasive PET/CT imaging using a CXCR4 radioligand revealed enlarged med-LNs with increased cellularity in MI-patients. Notably, the med-LN alterations observed in MI patients correlated with the infarct size and cardiac function. Taken together, the results obtained in our study provide evidence showing that MI-context induces pro-healing T cell autoimmunity in mice and confirms the existence of an analogous heart/med-LN/T cell axis in MI patients.

Graphical Abstract

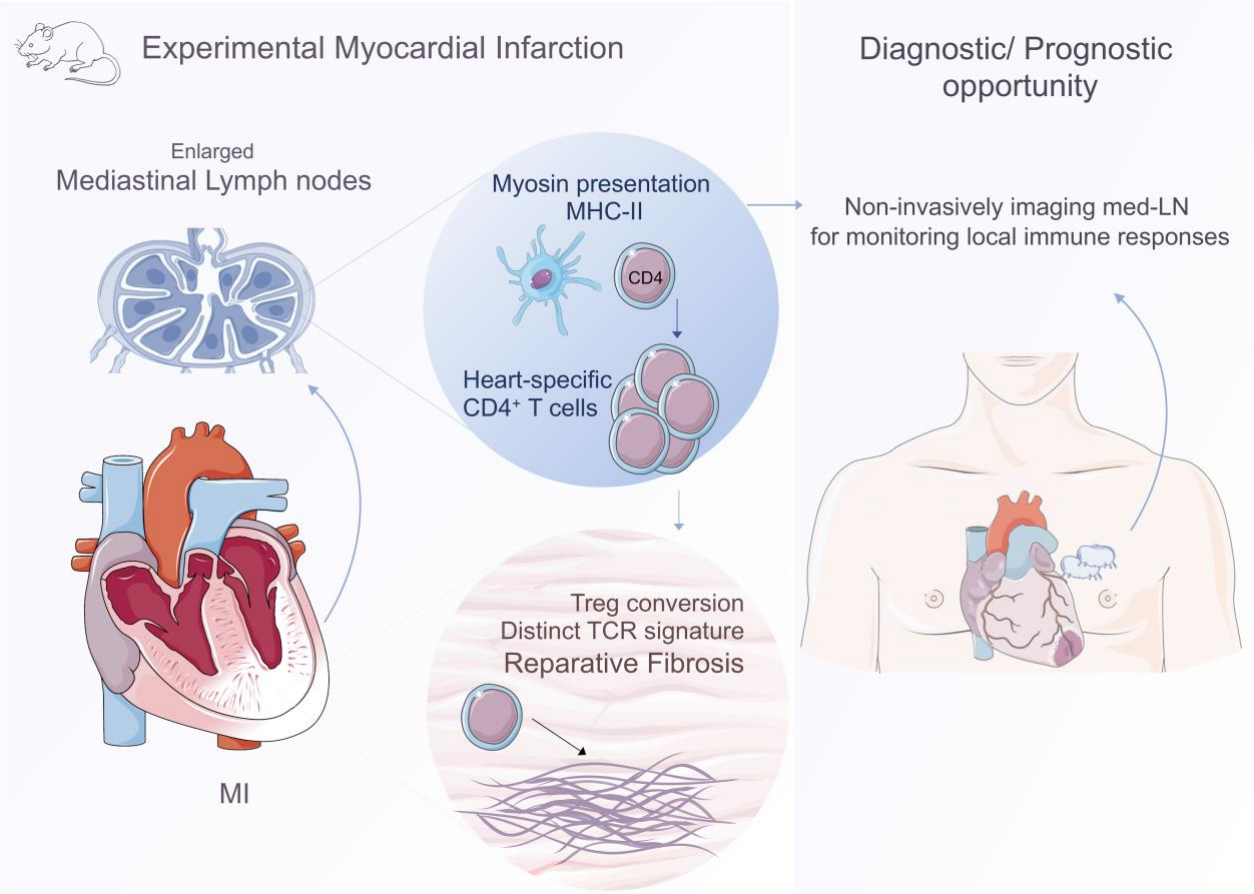

Introduction

Cardiology and immunology are disciplines born apart with different goals and tenets. Notwithstanding, a fertile association between these areas of knowledge has recently flourished, and leukocytes have now been implicated in the control of cardiac metabolism (1), rhythm (2, 3), aging (4), and repair (5-8). The contribution of immunological phenomena to cardiac repair is of particular clinical relevance because myocardial infarction (MI) is the leading cause of death worldwide (9). In addition to causing a life-threatening hemodynamic imbalance, the myocardial injury triggered by ischemia imposes a healing challenge on the heart, which is a terminally differentiated organ. Thus, many patients surviving an acute MI episode subsequently develop chronic heart failure (HF) due to maladaptive myocardial repair (10). Hence, there is an unmet need to better understand and eventually modulate the immune-inflammatory mechanisms underlying the myocardial healing process.

T lymphocytes are major players in the mediation of tissue repair, including that of cardiac injury (11-14). The participation of T cells in myocardial inflammation and repair has been observed in many organisms, ranging from fishes (14) to mammals (15-19), indicating that it is an evolutionarily conserved phenomenon. Previous studies from our group and others indicated that $CD4^+$ T cells become primed and proliferate in the mediastinal lymph nodes (med-LNs, heart-draining LNs) of infarcted mice and then infiltrate the myocardium (16, 18, 20, 21). Independent groups have reported that the regulatory T cells (Treg cells, defined as $FOXP3^+$) activated after MI exert salutary effects by accelerating the resolution of inflammation and promoting appropriate extracellular matrix deposition in the myocardial scar (14, 18, 20, 22, 23). Conventional T helper cells (Tconv cells, defined as $FOXP3^-$) have also been shown to positively influence the molecular milieu in the infarcted myocardium via a mechanism that depends on the extracellular purinergic metabolism (24).

T cell reactivity can benefit myocardial healing in mice by promoting reparative fibrosis in a postmitotic organ. However, sustained T cell responses in the heart can also fuel adverse remodeling and contribute to the progression of ischemic HF at later chronic stages (19). Furthermore, chronic T cell activation in the myocardium has also been shown to be detrimental in experimental models of pressure-overload-induced HF and during aging (4, 25-27). Taken together, these findings indicate that the crosstalk between T cells and the heart can exhibit a broad spectrum of possible outcomes in mice, depending on the context of activation and the timing of these responses. Furthermore, whether post-MI T cell responses are driven by cardiac antigens or by the recognition of danger-associated molecular patterns in the context of a particular cytokine milieu has not yet established. Most importantly, the translational relevance of this heart/T cell axis has not yet been fully confirmed in a meaningful clinical setting, mainly due to the challenges of obtaining samples from relevant sites other than peripheral blood, such as the myocardium and draining LNs (28).

In this study, we sought to elucidate the principles governing T cell activation, differentiation and functionality in the context of experimental MI (EMI) and to monitor the distribution of T cells in the heart and med-LNs of MI patients. Through a combination of unbiased screening with hypothesis-driven approaches, we identified an antigen-specific mode of T cell activation and revealed that the myocardium imposes an activation context that promotes the development of heart-specific T helper cells poised to exhibit a cardioprotective phenotype during the healing stage. Moreover, we combined histological analyses of myocardial autopsies with thoracic positron emission tomography/computed tomography (PET/CT) imaging using the novel radiotracer [^{68}Ga]Pentixafor, a ligand for C-X-C motif chemokine receptor 4 (CXCR4), and our results provide strong clinical evidence showing that a heart/T cell axis is also active in MI patients.

Results

Myosin heavy chain alpha (MYHCA) is a dominant cardiac antigen that triggers T helper cell activation after EMI

The proteins released by cardiomyocyte death during an ischemic event can be a source of antigens that stimulate adaptive immune cells. Thus, we sought to verify whether post-MI $CD4^+$ T cell responses are heart-specific and to eventually identify relevant cardiac epitopes. We tested the reactivity profile of $CD4^+$ T cells purified from infarcted mice against a library of 153 peptides covering the eight most relevant heart-enriched proteins encoded by mRNAs with > 5-levels in the heart compared with those in all other tissues, as detailed in the Human Protein Atlas (29). The cardiac proteins selected herein include sarcomere elements (alpha actin-1, myosin-binding protein C3, myosin heavy chain alpha, myosin light chain 2, troponin I3, and troponin T2), a cardiac receptor (adrenergic receptor beta 1), and a mitochondrial component (heat-shock protein family B3). The specific peptides (15 mers, Supplemental Table I) were selected based on in silico simulation of their major histocompatibility complex-II (MHC-II) binding properties (30).

As shown in Figure 1A-E, splenocytes purified from infarcted (but not from sham-operated) mice showed interleukin-2 (IL-2) response to MYHCA-derived epitopes, which is considered a readout for antigen-specific stimulation. No IL-2 response was observed with the T cells challenged with all other tested peptides, revealing that MYHCA is a dominant cardiac antigen in the MI-context. This heart-specific myosin isoform has already been implicated in the pathogenesis of experimental autoimmune myocarditis, and previous studies identified a specific MHC-II-restricted epitope ($MYHCA_{614-628}$) that is relevant in that disease model (31, 32). As shown in Figures 1A, 1C, and 1E, this single $MYHCA_{614-628}$ peptide could recapitulate similar T

cell responses in infarcted mice. The results revealed no response to a control peptide representing an irrelevant antigen (ovalbumin, $OVA_{323-339}$), and no interferon gamma (IFN-γ) response was observed to any of the peptides tested, including MYHCA (Figure 1A).

Cardiac-myosin-specific T helper cells (TCR-M) selectively accumulate in the infarcted heart and acquire a regulatory phenotype

After identifying $MYHCA_{614-628}$ as a crucial cardiac antigen that triggers the activation of T helper cells in the MI context, we sought to monitor the in vivo distribution and activation profile of MYHCA-specific T cells in infarcted mice. To that end, $5x10^6$ Thy1.1 MYHCA-specific cells were adoptively transferred into Thy1.2 syngeneic wild-type (WT) recipients prior to the induction of EMI, and their distribution and activation profile were monitored by flow cytometry (Figure 2, Supplemental Figure 1). These cells were obtained from a mouse strain exclusively bearing transgenic TCRs specific for the immunogenic MYHCA peptide ($MYHCA_{614-629}$) presented in the MHC-II context (henceforth termed TCR-M cells (33), generated by the co-authors B.L, and C.G.C.). Monoclonal TCR-M cells were defined as $CD4^+$ $TCR\beta^+$ $Thy1.1^+$ $TCV\alpha2^+$ singlets. Polyclonal endogenous T helper cells (ENDO cells) were defined as $CD4^+$ $TCR\beta^+$ $Thy1.1^-$ singlets. As shown in Figure 2B, TCR-M cells selectively accumulated in the heart and med-LNs of infarcted mice at the peak of the wound healing phase (day 7). The TCR-M cells vanished during a later chronic phase, indicating that post-MI autoreactivity to cardiac myosin is a self-limiting phenomenon (Figure 2C). Light-sheet fluorescence microscopy (LSFM) of whole unsliced hearts confirmed that TCR-M cells accumulate within the infarct zone but not in the healthy remote myocardium (Figures 2D-2E, Supplemental Video 1). The results revealed no antigen-specific T cell accumulation at day 49 post-MI (Figure 2F).

MI also had a major impact on the differentiation of TCR-M cells. When transferred into the MI context, TCR-M cells exhibited increased levels of CD44 surface expression at all sites compared with their baseline (i.e., pretransfer) expression levels (Figures 2G-2I). The frequency of $CD44^+$ differentiated cells was also higher among MI-TCR-M cells than in the endogenous $CD4^+$ T cell compartment (ENDO cells) at all analyzed sites ($P<0.05$). No CD44 upregulation was observed in the TCR-M cells found in the si-LNs of sham-operated mice (Figure 2G). However, the TCR-M cells isolated from the med-LNs of both MI and sham-operated mice displayed markers of cell activation (Figure 2H). These findings suggest that MYHCA is constitutively presented to $CD4^+$ T cells in the heart-draining LNs of healthy mice, even in the absence of cardiac damage, as previously reported (21, 34). TCR-M cells were virtually absent from sham-operated hearts, but they exhibited a differentiated phenotype in infarcted hearts (Figure 2I). A similar pattern was observed for FOXP3 expression. Notably, 55.2% of the TCR-M cells in the infarcted hearts were $FOXP3^+$, which is in sharp contrast to the baseline frequency (8.8%).

To better understand the mechanisms underlying the accumulation of $FOXP3^+$ TCR-M cells in the heart, we transferred Treg ($CD25^+$, $FOXP3^+$) and Tconv ($CD25^-$, $FOXP3^-$) TCR-M cells labeled with distinct, subset-specific, fluorescent intracellular tracers (Figure 3A). Flow cytometry analyses performed on day 7 post-MI confirmed that both T-cell subsets strongly proliferated in the heart and med-LNs, but not in the si-LNs, of infarcted mice (Figure 3 B-D). These results confirm that post-MI T-cell responses are largely driven by MYHCA-derived antigens. Remarkably, more than 50% of the TCR-M cells labeled as Tconv prior to cell transfer acquired $FOXP3^+$ expression in the myocardium, but not in the LNs, indicating that in situ Treg-conversion is the major factor driving Treg accumulation in the myocardial tissue (Figure 3B). Myosin-specific T cells also underwent in situ Treg-conversion in the absence of myocardial

infarction (Figure 3B), but the numbers of TCR-M cells found in the infarcted hearts were typically higher as compared to shams (Figure 2 B, L). Taken together, these results indicate that MI promotes the activation and recruitment of heart-specific T helper cells, and that the myocardial context induces myosin-specific T cells to acquire a Treg phenotype.

Antigen-specific T helper cells activated in the MI context acquire a nonclassical gene expression signature enriched with pro-healing factors

To better characterize how the MI context shapes the differentiation of antigen-specific $CD4^+$ T cells, we subsequently sorted TCR-M and ENDO cells from the med-LNs of infarcted vs sham-operated mice (day 7) for downstream gene expression profiling (Figure 4, Supplemental Figure 2).

The TCR-M cells were purified by fluorescence-activated cell sorting (FACS) and defined as $CD4^+$ $TCR\beta^+$ $Thy1.1^+$ $TCV\alpha2^+$ singlets, whereas the ENDO cells were defined as $CD4^+$ $TCR\beta^+$ $Thy1.1^-$ singlets. As shown in Figure 4A, the TCR-M and ENDO cell compartments displayed contrasting gene expression patterns in response to MI. After MI, the ENDO compartment, primarily composed of polyclonal cells, showed 236 downregulated genes but only 43 upregulated genes (> 2-fold difference compared with the sham counterpart, $P<0.05$). These findings reveal that, despite patent inflammation, MI imposes a largely inhibitory context on most polyclonal T cells. In sharp contrast, the TCR-M cells exhibited 153 upregulated and only 38 downregulated transcripts in response to MI, confirming that MI promotes the stimulation of heart-specific T helper cells.

The TCR-M cells activated in the MI context display a unique gene expression profile enriched with growth factors and pro-healing mediators but not with cytokines related to the classical T helper subsets. A list of the top 100 regulated transcripts is presented in Supplemental

Figure 2, and the top 30 regulated genes are shown in Figure 4C. Enrichment pathway analyses indicated that transcripts related to T cell trafficking within LNs (sphingosine 1-phosphate pathway), the TCR signaling cascade, and responses to hypoxic stress were particularly upregulated in TCR-M cells after MI (Figure 4D, and Supplemental Table II, $P<0.05$). Regarding the molecular function of TCR-M, unsupervised analyses identified M-CSF- receptor binding, chemokine receptor binding, IL-4 receptor binding, TGF-ß- receptor binding, IL-1 receptor binding, and growth factor activity among the top regulated transcription response patterns in TCR-M cells that are activated after MI (Figure 4D, Supplemental Figure 3, and Supplemental Table III, $P<0.05$).

Notably, most of the genes related to classically polarized T helper cells (e.g., *Ifng, Tnf, Il13* and *Il17*) were not differentially expressed in TCR-M cells activated after MI (Supplemental Figure 3). Notwithstanding, in response to MI, TCR-M, but not ENDO, cells significantly upregulated a unique set of growth factors and pro-healing mediators, such as *Csf1, Angptl2, Grn, Tgfb3* and *Fgf2* (Figure 4E, $P<0.05$). Moreover, TCR-M cells that were stimulated post-MI selectively showed unregulated expression levels of inhibitory checkpoint receptors such as *Tigit, Pdcd1, Ctla4* and *Btla* (Figure 4E, $P<0.05$). Moreover, these cells were particularly enriched with transcripts related to extracellular purinergic metabolism (*Cd38, Nt5e,* and *Entpd1*) and signaling (*P2rx4* and *P2rx7,* Figure 4E).Taken together, transcriptome profiling revealed that the MI context imposes an inhibitory tonus on polyclonal ENDO cells but favors the development of heart-specific T cells with a distinct gene expression profile.

Heart-specific CD4$^+$ T cells activated in the MI context exert cardioprotective effects

Next, we evaluated the post-MI inflammation and repair processes in mice receiving adoptive transfer of MYHCA- versus ovalbumin (OVA)-specific T helper cells (TCR-M and

DO11.10 respectively, Figure 5A). We used Ova-specific T cells as a control because Ova is not an autoantigen in mice and hence irrelevant in the MI context. In these experiments, we enrolled DO11.10 mice as recipients (35) for the sake of excluding any possible effects of endogenous antigen-specific T helper cells. The specificity of the transferred $CD4^+$ T cells had no impact on the infarct size (Figure 5B, day 7 post-MI), heart-to-body weight, wet and dry lung-to-body weight, and absolute numbers of cardiac leukocytes (Supplemental Figure 4A-C, day 5 post-MI). However, echocardiography analyses performed on day 7 post-MI revealed that hearts enriched with autoreactive $CD4^+$ T cells presented a better preserved fractional area change, which serves as a readout for improved systolic function (Figure 5C, $P<0.05$). Similar findings were observed for the end-systolic area measurement ($P= 0.074$, Figure 5D), but no in the end-diastolic area were observed (Figure 5E). Mechanistically, we found that the adoptive transfer of TCR-M cells promoted an increased accumulation of pro-fibrotic MHC-$II^{hi}CCR2^{lo}$ macrophages (36) on day 5 post-MI (Figure 5F, Supplemental Figure 4E), compared to DO11.10 cell treatment. Histological analyses of the infarct zone revealed a higher collagen content in the scars TCR-M-treated mice, as quantified by Picrosirius red staining and collagen-III immunofluorescence staining (Figure 5 G-H, $P< 0.05$).

To complement this approach, we also transferred WT lymphocytes purified from the med-LN of sham vs infarcted mice into lymphocyte-deficient animals and then monitored cardiac function in the recipients (Supplemental Figure 5). These experiments were performed because previous studies have established that the transfer of T cells from diseased mice can produce cardiac injury in unchallenged recipients (34). In contrast to the autoimmune myocarditis context, we did not observe any signs of myocardial-injury mediated by the lymphocytes obtained from MI-donors (Supplemental Figure 5B-5E). These findings further support the notion that post-MI T-cell autoimmunity is not pathogenic during the early healing phase.

$CD4^+$ T cells infiltrating the murine infarcted myocardium exhibit a distinct repertoire signature

After showing that T cells specific for a prototypic myocardial antigen promote myocardial healing via an adoptive transfer approach, we aimed to further confirm whether the endogenous T cell response is autoantigen-dependent. The fundamental role of T cells in adaptive immunity relies mainly on a diverse repertoire of T cell receptor (TCR) α and β chains that display unique antigen specificities. Thus, we performed high-throughput sequencing of the of TCRβ complementary determining region 3 (CDR3β) on $CD4^+$ T cells purified by FACS from the heart and med-LNs of MI and sham-operated mice (Figure 6A, and Supplemental Figure 6A) as an unbiased approach to screen for MI-related TCR signatures. As shown in Figures 6B-6D, the $CD4^+$ T cells infiltrating the infarcted myocardium exhibited a skewed repertoire dominated by a restricted set of TCR sequences. In the tree maps presented in Figure 6B, each colored spot represents a unique TCRβ CDR3 sequence (a T cell clone), and the size of each spot denotes its relative frequency. The unevenness of the spots observed in the cardiac T cell samples and the high frequencies found for some sequences (37) indicated the clonal expansion of these cells. The Gini inequality coefficient was further calculated as an indicator of the repertoire evenness and clonal dominance (Figure 6C, Supplemental Figure 6B): a Gini coefficient value of 0 denotes an even repertoire in which every sequence is present in equal abundance, whereas a value of 1 indicates that the repertoire is dominated by a single sequence (38, 39). Notably, the cardiac T cells displayed the highest Gini scores among all the groups (Figure 6C, $P<0.05$), which further indicates that the post-MI T cell responses are marked by oligoclonal expansions. Because the pool of T cells found in tissues was considerably smaller than that in LNs, we also assessed the Gini coefficient for a subsampling of equal size in each group (Supplemental Figure 6B). The observations remained unaltered also under these conditions. Heart T cells also had a much less

diverse repertoire than that found in LNs, as assessed using Simpson's diversity index (Figure 6D, Supplemental Figure 6B). Most strikingly, T cells infiltrating the infarcted myocardium exhibited a unique repertoire signature, as evidenced by several factors. First, the MI-related cardiac TCR repertoire was marked by a particular usage of variable (TRBV) and joining (TRBJ) gene segments (Figure 6E-6F, and Supplemental Figure 6E). In particular, TRBV19 was significantly expanded in MI-related cardiac T cells compared with its usage in the med-LNs, whereas the usage of TRBV5 was significantly reduced (Figure 6E, $P<0.05$). Second, the CDR3 length distribution of TRBV19 sequences was skewed in the heart samples, whereas a Gaussian distribution was found in the LN samples (Supplemental Figure 6D). Because V-J recombination is a random process, the length distribution of natural repertoires tends to exhibit a Gaussian distribution. Therefore, biases in the distribution of TCRβ CDR3 lengths are indicative of clonal expansions (40). Third, MI-related T cells had a unique pool of sequences exhibiting minimal overlap with all the other samples investigated herein (Figure 6G, and Supplemental Figure 6F).

The identity of cognate antigens cannot be directly extrapolated from the TCR sequence data. Therefore, we also assessed the TCR repertoire of $CD4^+$ T cells purified from the axillary LNs (ax-LNs) of mice that were subcutaneously immunized with cardiac myosin and heart extract (in adjuvants) because these repertoires were expected to be enriched in heart-specific sequences upon specific immunization. As a control, we also assessed the ax-LN TCR repertoire in mice that received subcutaneous administration of the adjuvant alone. The high degree of clonality exhibited by the cardiac T cell pool remained statistically significant compared with that found for all ax-LN repertoires, even those from immunized mice (Supplemental Figures 7A-7E). Notably, the T helper cell repertoire found in the ax-LNs of mice that received heart extract immunization also exhibited an increased TRBV19:TRBV5 ratio, similar to that found for cardiac T cells and in sharp contrast to that found for the control ax-LNs (Supplemental Figures

7F-G). Notwithstanding, the comparison of the TCRβ CDR3 sequences in the infarcted and immunized groups revealed no significant repertoire overlap. To a great extent, this result might be related to the fact that the cardiac T cell repertoire is largely composed of private sequences (i.e., no CDR3 repertoire overlap between individual cardiac EMI samples).

Taken together, the results from this unbiased screening approach revealed that the $CD4^+$ T cells infiltrating the infarcted myocardium display a distinct T cell repertoire signature dominated by a limited set of expanded clones. These characteristics are hallmarks of antigen-driven responses.

Evidence for a heart/T cell axis in MI patients

We subsequently sought to assess the existence of a putative heart/T cell axis in MI patients. Our EMI findings showed that the most important T cells are in either the heart or the med-LNs (heart-draining LNs) rather than in the periphery. To validate these findings, we assessed the presence of $FOXP3^+$ and $CD4^+$ cells in cardiac autopsies. Twenty-three patients were diagnosed at autopsy with recent MI in the left ventricle. These MI patients were further categorized into three distinct reaction phases. The early phase (~3-12 hours post-MI) is marked by lactate dehydrogenase (LDH) decoloration without neutrophilic cell infiltration (n=6). In the inflammatory phase (12 hours to 5 days post-MI), neutrophilic granulocytes are particularly observed in the infarcted myocardium (n=9), whereas in the proliferation phase (5-14 days post-MI), the formation of a granulation tissue is obvious (n=8). Nine patients without pathological evidence of MI-related death were included as controls. A description of patients from whom cardiac autopsies were obtained is presented in Supplemental Table IV. As shown in Figures 7A-7E, $CD4^+$ and $FOXP3^+$ cells were found in the infarcted hearts, and their levels peaked during the

proliferative phase of wound healing ($P<0.05$). Neither $CD4^+$ nor $FOXP3^+$ cells were found in the control hearts.

Several mouse studies have shown that T cells infiltrating the injured myocardium are activated in and originate from the med-LNs (16, 17, 25), suggesting that assessing the med-LN morphology and cellularity in MI patients could also yield clinically relevant information. Thus, we acquired thoracic CT images from MI patients to assess the med-LN morphology. Moreover, we combined CT with PET imaging, using a radiolabeled CXCR4 ligand ([^{68}Ga]Pentixafor). CXCR4 is a chemokine receptor that is constitutively expressed at high levels on T cells and regulates their migration along gradients of the chemokine CXCL12 (41). CXCR4 is also expressed on some monocyte subsets (42), on B cell subsets (43), and on hematopoietic stem cells (44), which are present at only small frequencies within LNs. A flow cytometry analysis of the CXCR4 distribution across different leukocyte subsets in mice confirmed that T cells account for more than 90% of the $CXCR4^+$ cells in med-LNs but less than 15% of the $CXCR4^+$ cells in the heart (Supplemental Figure 8). We therefore employed a noninvasive CXCR4 monitoring strategy to obtain a readout for T cellularity in heart-draining LNs. Nonmalignant Conn's adenoma patients who had received [^{68}Ga]Pentixafor-PET/CTs for diagnostic work-up were included as controls. Conn's adenomas are aldosterone-producing benign conditions that account for 30-40% of all cases of primary aldosteronism. Because these adenomas overexpress CXCR4 (45), these patients were subjected to receptor-directed imaging as part of an endocrinological investigation, and none of these patients presented elevated serum levels of C-reactive protein (<0.5 mg/dl).

As shown in Figures 7F-7G, the med-LNs were significantly enlarged in MI patients but not in the control group (19.1±7.6 mm versus 11.7±4.2 mm; $P<0.05$, measured at day 7 post-MI,

range 2-13 days). The MI patients also exhibited significantly increased CXCR4 expression in the med-LNs compared with the control patients (as derived by [^{68}Ga]Pentixafor-PET/CT; SUV_{max}, 2.7±0.9 versus 1.9±0.3, P<0.001, Figures 7G-7I). These findings indicated that the med-LN enlargement observed in MI patients might be, at least in part, related to local expansion in the T cell compartment. Furthermore, the size of the med-LNs showed a moderate correlation with the infarct volume derived by cardiac magnetic resonance (CMR, r=0.45, P=0.05, Supplemental Figure 9A) and with the levels of serum creatine kinase after MI (sum of CK, r=0.57, P<0.01; Supplemental Figure 9B). The uptake of [^{68}Ga]Pentixafor in the med-LNs was positively correlated with CXCR4 expression in the infarcted myocardium (r=0.52, P=0.03, Supplemental Figure 9C). Moreover, the CXCR4 signal in the med-LNs suggested a positive prognosis with smaller myocardial necrosis volumes in a follow-up CMR (median 4 months after MI, r=-0.51, P=0.06, Supplemental Figure 9D). Taken together, these clinical findings reveal for the first time the existence of a local heart/med-LN/T cell axis in MI patients and show remarkable similarities with the observations performed in the framework of EMI.

Discussion

Emerging concepts in the field of cardiology suggest that the infarcted myocardium could be perceived as a wounded tissue (46), and hence, the immunological phenomena underlying myocardial repair have received considerable attention worldwide (e.g. (5, 8, 47-51). The contribution of innate immune mechanisms to post-MI inflammation, healing and remodeling has been well scrutinized over the past two decades (52, 53), but the involvement of the adaptive arm of the immune system has only recently been recognized (8, 16, 18, 20, 22, 54, 55). In this study, we assessed global features of the post-MI T cell repertoire and pinpointed a defined cardiac

antigen that is targeted by $CD4^+$ T cells after EMI to dissect the bidirectional cardio-immune crosstalk in unprecedented detail. Moreover, through a combination of histological analyses of cardiac tissue samples with noninvasive imaging of the med-LNs in MI patients, we provide compelling evidence showing such a heart/T cell axis might hold great translational implications.

T cells reportedly influence cardiac injury, repair, and remodeling in various organisms, ranging from fishes to mammals (16, 18-21, 56). Notwithstanding, the question of whether post-MI autoimmune responses exert salutary or detrimental effects has remained debated (54). Independent laboratories have recently reported that T cells may foster early cardiac healing by modulating macrophage polarization (18), fibroblast activity (20), and extracellular purinergic metabolism (21). However, chronic T cell activation in the myocardium has also been reported to fuel the development of adverse remodeling in models of ischemic and stress-overload-induced HF (19, 25-27). Moreover, the reactivity profile of T cells activated in the MI context has not yet been assessed, and whether these cells target specific antigens released by dying cardiomyocytes or simply respond to the inflammatory milieu remains largely unclear (57).

Herein, we found that T cells infiltrating the infarcted myocardium display a unique repertoire signature marked by a preferential expansion of TCRBV19-expressing clones. Notably, a similar bias toward the use of TRBV19 gene segments was also observed in mice immunized with cardiac antigens. In a previous study, Hu et al. (58) also observed skewed $TRBV19^+$ T cell responses in a murine model of cardiac allograft transplant. Furthermore, Klingenberg et al. (59), Heidecker et al. (60), and Blohm et al. (61) independently reported elevated TCRBV19 expression in coronary thrombi obtained from patients with coronary syndrome, and in cardiac biopsies obtained from patients with autoimmune myocarditis and dilative cardiomyopathy respectively. Taken together, these findings strongly suggest that $TRBV19^+$ T cells might be associated with heart-specific T cell responses in different organisms,

ranging from mice to men. The causes underlying this remarkable association between specific TRβV usage and cardiotropic immune responses remain unclear, but the converging evidence might encourage future research aiming to elucidate this point.

In the present study, we identified cardiac myosin (MYHCA) as a dominant cardiac antigen in the MI context and established a defined system for dissecting the role of MYHCA-specific T cell responses in the wounded myocardium in unprecedented detail. MYHCA is a prototypical cardiac antigen for several reasons: it is selectively expressed in the myocardium but not in any other tissue (31, 62); it is constitutively processed and presented to T cells by cardiac antigen-presenting cells (34); in contrast to most tissue-restricted proteins, MYHCA is not expressed by thymic epithelial cells, meaning that central tolerance to this cardiac antigen is absent/impaired (63); and it has been strongly implicated in the pathogenesis of autoimmune myocarditis (33).

In addition to specificity, our data reveal that the myocardial milieu dictates T cell phenotypic polarization favoring the in situ induction of Treg cells and the development of protective autoimmune responses that benefit tissue repair through the promotion of collagen deposition. The latter findings are in accordance with those observed in our own previous study, which revealed that mice lacking $CD4^+$ T cells have impaired collagen deposition after EMI (16). The detailed mechanism underlying the T cell-mediated myocardial fibrosis process remains elusive, but our findings suggest that it might be dependent on crosstalk with MHC-$II^{hi}CCR2^{lo}$ macrophages, which are upregulated in TCR-M-transferred mice. Recent studies have established that MHC-$II^{hi}CCR2^{lo}$ macrophages exhibit a transcriptome profile enriched with pro-fibrotic genes, show lower metalloproteinase activity and are involved in the cardiac fibrosis process in models of diastolic dysfunction (36).

It is important to consider that the role of autoreactive T cells in MI and HF is likely stage-dependent. This is particularly relevant for the T cell mediated cardiac fibrosis. Building a solid and fast scar after MI helps preventing cardiac rupture and infarct expansion, but progressive collagen deposition can also lead to adverse remodeling (7). This might help explaining why cardiac $CD4^+$ T cells have been recently implicated in both salutary and pathogenic mechanism (16-28). Furthermore, it is important to recognize that TCR-M cells induce autoimmune myocarditis in donor mice (33). Together, these findings indicate that the outcome of heart autoimmunity is largely context-dependent and reveal an unprecedented role for the myocardial milieu in the shaping of T cell phenotypic polarization.

A similar dual role for T helper cells in mediating tissue-specific autoimmunity and repair was previously reported by Schwartz et al. (11). These authors observed that the same antigen-specific $CD4^+$ T cells that mediate experimental autoimmune encephalomyelitis can also foster spinal cord repair. Understanding the differences between physiological and pathogenic heart-specific autoimmunity might be a central issue to be scrutinized in future studies in this field.

To the best of our knowledge, we provide the first report of the existence of a heart/med-LN/T cell axis in MI patients. Moderate infiltration of $CD4^+$ and $FOXP3^+$ cells is consistently observed in the infarcted myocardia of mice and humans. The kinetics of cardiac T cell infiltration show substantial similarities across species, and the numbers of infiltrating cardiac T cells peak at the healing phase. MI patients also exhibit alterations in their med-LN morphology and cellular composition similar to those observed in rodents (16, 17, 24). CT measurements provided valuable information of the med-LN morphology but cannot aid the discrimination of alterations due to edema from those due to increased cellularity. Therefore, the critical advantage provided by combined CT/CXCR4 PET tracing is that this approach provides strong evidence for alterations due to increased cellularity, which is a hallmark of adaptive immune responses. We

acknowledge that the widespread distribution of CXCR4 expression across different cell types demands careful interpretation of these findings. However, the limited specificity of this target can be compensated by the anatomical specificity of our observations because lymphocytes account for the vast majority of cells within LNs (64).). It might therefore be safe to conclude that the PET/CT approach employed in this study might offer a suitable method for monitoring the *local* adaptive immune responses in MI patients. Indeed, a recently published study revealed that CXCR4 plays an important role in controlling T cell trafficking in the context of EMI and thereby influences the healing outcome (65) , and these findings provide great mechanistic support for our clinical findings.

The observed correlation between alterations in the med-LN and the clinical findings (e.g., infarct volume and follow-up cardiac function) reinforces the clinical relevance of this approach, and indicates that imaging the heart-draining LNs might provide additional valuable clinical information. This bold step might help overcome the limitations of peripheral blood sampling (only less than 2% of all lymphocytes are typically present in the peripheral blood (66) and might even allow the tailoring of directed immunotherapeutic interventions in the future.

Cardiologists can rely on good therapeutic and interventional options for the treatment of acute MI and for attenuating the progression of remodeling (9, 10), but no tools are currently available for fostering the myocardial healing processes that bridge these two conditions. In fact, prospectively validated biomarkers are currently not available for monitoring the quality of ongoing myocardial healing, and thus, clinicians cannot identify patients undergoing adverse remodeling until they reach a critical HF stage. Thus, there is an unmet need in the field of cardiology to better understand and eventually modulate the mechanisms underlying the myocardial repair process (8, 67). A new discipline at the crossroads between immunology and cardiology has rapidly flourished over the past decade with the aim of filling these gaps. From the

cardiological perspective, this multidisciplinary enterprise might offer novel and exciting opportunities for preventing the development of ischemic HF, which is a consequence of poor post-MI healing. From an immunological perspective, this association with cardiology might offer a unique opportunity to better understand the often-neglected aspects of physiological autoimmunity.

Materials and Methods

Due to space restrictions, detailed descriptions of the experimental methods are provided in Supplementary Materials.

Study design

Mouse studies: Our aim was to clarify the functional significance of autoreactive T cell responses to EMI. Therefore, we selected a model of transgenic murine cardiac myosin-specific $CD4^+$ T cells (TCR-M) that were adoptively transferred into wild-type and DO11.10 recipient mice prior to the induction of EMI through permanent surgical ligation of the left coronary artery. The recipient DO11.10 mice were selected in some experiments because the entire $CD4^+$ T cell compartment in these animals is composed of ovalbumin-specific cells (i.e., an irrelevant antigen in the MI context). The distribution and differentiation of endogenous and transferred T cells were analyzed by flow cytometry and transcriptome analysis of sorted cells. Echocardiography was performed to characterize the clinical phenotype of the animals. To further study the role of endogenous lymphocytes activated in the MI context, bulk med-LN-derived cells were adoptively transferred into naïve lymphocyte-deficient Rag1-KO mice. Furthermore, we performed an analysis of the TCR repertoire using a T cell receptor sequencing approach to confirm the clonal expansion of endogenous T cells in response to MI.

The echocardiographic imaging data were evaluated by a blinded experimenter. The exclusion criteria were set a priori according to the heart rate during echocardiography (heart rate >450 beats per minute), and the FACS cell yields were too low to draw reliable conclusions. Outliers were not excluded from the statistical analyses.

Human studies: The translational relevance of the murine findings obtained in the current study was tested in a clinical setting using histological and imaging approaches. $CD4^+$ and $FOXP3^+$ T cells on immunohistological slices of myocardial autopsy samples from patients that died at various time points after MI were quantified as previously described (68). Furthermore, nine patients for whom there was no pathological evidence of death from a cause related to MI were included as controls. Furthermore, we reexamined existing PET/CT datasets from patients who recently suffered from MI and from patients without heart disease using a novel CXCR4-specific radioligand and depicted its expression in both med-LNs and the myocardium (69). Five patients who underwent CXCR4-directed PET/CT due to suspicion of benign Conn's adenoma were included as controls. Detailed patient information is provided in Supplemental Tables IV and V.

Statistical analyses

Graphs of the data obtained from all the EMI studies were prepared to display the group mean values (bars), the standard errors of the mean (SEMs), and the distributions of each individual value. Statistical analyses were performed using GraphPad Prism software (Version 7.0d, GraphPad Software, Inc.), as described in each figure legend, and the TCR-seq data were statistically analyzed using MATLAB 2017a (MathWorks, Inc.). A P value less than 0.05 was considered statistically significant.

The statistical analyses of the data obtained from the clinical studies were performed using Statistical Packages for Social Sciences software (IBM SPSS 22.0.0.0, IBM Corp.). The

data were tested for normality using Levene's test and were found to not be normally distributed. Differences between groups containing continuous data were tested using the Mann-Whitney U test, unless otherwise indicated. Fisher's exact test and the Freeman-Halton extension of Fisher's exact test were used to test the associations between categorical data. The results were considered to be significantly different if the two-sided *P* value was less than 0.05. The data are presented as box plots showing the medians, 25^{th}-75^{th} percentiles (boxes) and 5^{th}-95^{th} percentiles (whiskers).

Study Approval

All animal procedures were approved by the local authorities (Landesverwaltungsamt Sachsen-Anhalt, Halle, Germany; and Regierung von Unterfranken, Würzburg, Germany) and were performed according to the guidelines of the Federation for Laboratory Animal Science Associations (FELASA) (70, 71).

The investigation performed on human autopsies was approved by and performed according to the guidelines of the ethics committee of Amsterdam UMC, location VUmc (Amsterdam Medical Center, Amsterdam, the Netherlands), which conformed to the Declaration of Helsinki. [68Ga] Pentixafor was administered clinically on a compassionate use basis in compliance with §37 of the Declaration of Helsinki, the German Medicinal Products Act, AMG §13 2b and in accordance with the responsible regulatory body (Regierung von Oberfranken, Bayreuth, Germany). All patients gave written informed consent prior to imaging. Due to the retrospective nature of this study, the local institutional review board of University Hospital Würzburg waived the requirement for additional approval.

Author contributions: C.G. performed the epitope mapping experiments. M.R., M.dG, G.R. performed the cell transfers, murine surgeries and echocardiography. M.dG., M.R., C.K., and G.R. performed the experiments and analyzed the data (immunization, flow cytometry, FACS, and histology). P.S. and G.R. performed the transcriptomic analyses and analyzed the transcriptome readouts. G.R., M.R., S.F. and U.H. designed the murine studies. K.G.H. and L.B. analyzed the LSFM samples. H.W.M.N., E.t.H., P.A.J.K., A.M.vdL. and J.J.P. acquired and analyzed the human MI autopsies; C.L. and M.K. acquired and analyzed the PET/CT data; and W.R.B. and T.R. acquired and analyzed the CMR imaging data. N.F. and D.R. analyzed the TCR data, and C.G.C. and B.L. generated the TCR-M mouse strain and contributed to the interpretation of the data. All the coauthors contributed to the preparation of the manuscript.

Acknowledgments: We greatly appreciate the excellent technical assistance of Susanne Koch, Claudia Pilowski, Helga Wagner, Andrea Leupold, Elena Vogel, Jürgen Pinnecker, Mike Friedrich, Dr. Alexander Navarrete-Santos, and Dr. Vesselin Christov and the theoretical contributions provided by Prof. Gottfried Alber and Prof. Emer. Dr. Nelson Vaz. The Graphical Abstract Figure has been prepared with the help of Servier Medical Art. **Funding sources:** G.R. received funding from the Interdisciplinary Center for Clinical Research-Würzburg (IZKF-Würzburg, E-354), from the Marija-Orlovic Foundation, and from the European Research Area Network- Cardiovascular Diseases (ERA-NET-CVD JCT2018, AIR-MI consortium); U.H. received funding from the Deutsche Forschungsgemeinschaft (SFB688, TPA10); and K.G.H. received funding from the Rudolf-Virchow Center. C.G. received a scholarship from the Deutsche Herzstiftung, and L.B. received a scholarship from the Deutsche Gesellschaft für Kardiologie. N.F. is supported by the David and Fela Shapell Family Institute for Preclinical Studies and the Florence Blau Charitable Trust and is the incumbent of the Eugene and Marcia Applebaum Professorial Chair. **Competing interest:** HJW is the founder and a shareholder of

Scintomics, which provided the CXCR4 radiotracer. All the other authors declare that they have no competing interests. **Data and material availability:** The transcriptome data discussed in this study have been deposited in NCBI's Gene Expression Omnibus and are accessible through GEO Series accession number GSE116569 (https://www.ncbi.nlm.nih.gov/geo/query/acc.cgi?acc=GSE116569). Similarly, the TCR-seq data discussed herein are accessible through GEO Series accession number GSE117076 (https://www.ncbi.nlm.nih.gov/geo/query/acc.cgi?acc=GSE116569). The TCR-M mice utilized in this study are available under a material transfer agreement with Kantonsspital St. Galen.

Supplemental Materials:

Supplemental methods

Supplemental Figures 1, 2, 3, 4, 5, 6, 7, 8, and 9.

Supplemental Tables I, II, III, IV, and V.

Supplemental Movie 1.

References

1. Amit U, Kain D, Wagner A, Sahu A, Nevo-Caspi Y, Gonen N, et al. New role for interleukin-13 receptor α1 in myocardial homeostasis and heart failure. *Journal of the American Heart Association.* 2017;6(5).
2. Monnerat G, Alarcón ML, Vasconcellos LR, Hochman-Mendez C, Brasil G, Bassani RA, et al. Macrophage-dependent IL-1β production induces cardiac arrhythmias in diabetic mice. *Nature Communications.* 2016;7.
3. Hulsmans M, Clauss S, Xiao L, Aguirre AD, King KR, Hanley A, et al. Macrophages Facilitate Electrical Conduction in the Heart. *Cell.* 2017;169(3):510-22.e20.

4. Ramos GC, van den Berg A, Nunes-Silva V, Weirather J, Peters L, Burkard M, et al. Myocardial aging as a T-cell-mediated phenomenon. *Proc Natl Acad Sci U S A.* 2017;114(12):E2420-E9.

5. Hofmann U, and Frantz S. Role of lymphocytes in myocardial injury, healing, and remodeling after myocardial infarction. *Circ Res.* 2015;116(2):354-67.

6. Hofmann U, and Frantz S. Role of T-cells in myocardial infarction. *Eur Heart J.* 2016;37(11):873-9.

7. Ramos G, Hofmann U, and Frantz S. Myocardial fibrosis seen through the lenses of T-cell biology. *J Mol Cell Cardiol.* 2016;92:41-5.

8. Nunes-Silva V, Frantz S, and Ramos GC. Lymphocytes at the Heart of Wound Healing. *Adv Exp Med Biol.* 2017;1003:225-50.

9. Ibanez B, James S, Agewall S, Antunes MJ, Bucciarelli-Ducci C, Bueno H, et al. 2017 ESC Guidelines for the management of acute myocardial infarction in patients presenting with ST-segment elevation. *European Heart Journal.* 2018;39(2):119-77.

10. Ponikowski P, Voors AA, Anker SD, Bueno H, Cleland JGF, Coats AJS, et al. 2016 ESC Guidelines for the diagnosis and treatment of acute and chronic heart failure The Task Force for the diagnosis and treatment of acute and chronic heart failure of the European Society of Cardiology (ESC) Developed with the special contribution of. *European Heart Journal.* 2016:891-975.

11. Schwartz M, Moalem G, Leibowitz-Amit R, and Cohen IR. Innate and adaptive immune responses can be beneficial for CNS repair. *Trends in Neurosciences.* 1999;22(7):295-9.

12. Harty M, Neff AW, King MW, and Mescher AL. Regeneration or scarring: An immunologic perspective. *Developmental Dynamics.* 2003;226(2):268-79.

13. Burzyn D, Kuswanto W, Kolodin D, Shadrach JL, Cerletti M, Jang Y, et al. A Special Population of regulatory T Cells Potentiates muscle repair. *Cell.* 2013;155(6):1282-95.

14. Hui SP, Sheng DZ, Sugimoto K, Gonzalez-Rajal A, Nakagawa S, Hesselson D, et al. Zebrafish Regulatory T Cells Mediate Organ-Specific Regenerative Programs. *Developmental Cell.* 2017;43(6):659-72.e5.

15. Maisel A, Cesario D, Baird S, Rehman J, Haghighi P, and Carter S. Experimental autoimmune myocarditis produced by adoptive transfer of splenocytes after myocardial infarction. *Circulation Research.* 1998;82(4):458-63.

16. Hofmann U, Beyersdorf N, Weirather J, Podolskaya A, Bauersachs J, Ertl G, et al. Activation of CD4+ T lymphocytes improves wound healing and survival after experimental myocardial infarction in mice. *Circulation.* 2012;125(13):1652-63.

17. Ramos GC, Dalbo S, Leite DP, Goldfeder E, Carvalho CR, Vaz NM, et al. The autoimmune nature of post-infarct myocardial healing: oral tolerance to cardiac antigens as a novel strategy to improve cardiac healing. *Autoimmunity.* 2012;45(3):233-44.

18. Weirather J, Hofmann UD, Beyersdorf N, Ramos GC, Vogel B, Frey A, et al. FOXP3+ CD4+ T cells improve healing after myocardial infarction by modulating monocyte/macrophage differentiation. *Circ Res.* 2014;115(1):55-67.

19. Bansal SS, Ismahil MA, Goel M, Patel B, Hamid T, Rokosh G, et al. Activated T lymphocytes are essential drivers of pathological remodeling in ischemic heart failure. *Circulation: Heart Failure.* 2017;10(3).

20. Saxena A, Dobaczewski M, Rai V, Haque Z, Chen W, Li N, et al. Regulatory T cells are recruited in the infarcted mouse myocardium and may modulate fibroblast phenotype and function. *AJP: Heart and Circulatory Physiology.* 2014;307(8):H1233-H42.

21. Van der Borght K, Scott CL, Nindl V, Bouche A, Martens L, Sichien D, et al. Myocardial Infarction Primes Autoreactive T Cells through Activation of Dendritic Cells. *Cell Rep.* 2017;18(12):3005-17.

22. Tang TT, Yuan J, Zhu ZF, Zhang WC, Xiao H, Xia N, et al. Regulatory T cells ameliorate cardiac remodeling after myocardial infarction. *Basic Res Cardiol.* 2012;107(1):232.

23. Skorska A, von Haehling S, Ludwig M, Lux CA, Gaebel R, Kleiner G, et al. The CD4+AT2R+T cell subpopulation improves post-infarction remodelling and restores cardiac function. *Journal of Cellular and Molecular Medicine.* 2015;19(8):1975-85.

24. Borg N, Alter C, Gorldt N, Jacoby C, Ding Z, Steckel B, et al. CD73 on T Cells Orchestrates Cardiac Wound Healing After Myocardial Infarction by Purinergic Metabolic Reprogramming. *Circulation.* 2017;136(3):297-313.

25. Laroumanie F, Douin-Echinard V, Pozzo J, Lairez O, Tortosa F, Vinel C, et al. CD4+ T cells promote the transition from hypertrophy to heart failure during chronic pressure overload. *Circulation.* 2014;129(21):2111-24.

26. Nevers T, Salvador AM, Grodecki-Pena A, Knapp A, Velázquez F, Aronovitz M, et al. Left ventricular t-cell recruitment contributes to the pathogenesis of heart failure. *Circulation: Heart Failure.* 2015;8(4):776-87.

27. Kallikourdis M, Martini E, Carullo P, Sardi C, Roselli G, Greco CM, et al. T cell costimulation blockade blunts pressure overload-induced heart failure. *Nat Commun.* 2017;8:14680.

28. Boag SE, Das R, Shmeleva EV, Bagnall A, Egred M, Howard N, et al. T lymphocytes and fractalkine contribute to myocardial ischemia / reperfusion injury in patients. 2015;125(8):1-14.

29. Uhlen M, Fagerberg L, Hallstrom BM, Lindskog C, Oksvold P, Mardinoglu A, et al. Proteomics. Tissue-based map of the human proteome. *Science.* 2015;347(6220):1260419.

30. Wang P, Sidney J, Dow C, Mothe B, Sette A, and Peters B. A systematic assessment of MHC class II peptide binding predictions and evaluation of a consensus approach. *PLoS Comput Biol.* 2008;4(4):e1000048.

31. Pummerer CL, Luze K, Grässl G, Bachmaier K, Offner F, Burrell SK, et al. Identification of cardiac myosin peptides capable of inducing autoimmune myocarditis in BALB/c mice. *Journal of Clinical Investigation.* 1996;97(9):2057-62.

32. Krebs P, Kurrer MO, Kremer M, De Giuli R, Sonderegger I, Henke A, et al. Molecular mapping of autoimmune B cell responses in experimental myocarditis. *J Autoimmun.* 2007;28(4):224-33.

33. Nindl V, Maier R, Ratering D, De Giuli R, Zust R, Thiel V, et al. Cooperation of Th1 and Th17 cells determines transition from autoimmune myocarditis to dilated cardiomyopathy. *Eur J Immunol.* 2012;42(9):2311-21.

34. Smith SC, and Allen PM. Expression of myosin-class II major histocompatibility complexes in the normal myocardium occurs before induction of autoimmune myocarditis. *Proceedings of the National Academy of Sciences of the United States of America.* 1992;89(19):9131-5.

35. Murphy KM, Heimberger AB, and Loh DY. Induction by antigen of intrathymic apoptosis of CD4+CD8+TCRlo thymocytes in vivo. *Science.* 1990;250(4988):1720-3.

36. Hulsmans M, Sager HB, Roh JD, Valero-Munoz M, Houstis NE, Iwamoto Y, et al. Cardiac macrophages promote diastolic dysfunction. *J Exp Med.* 2018;215(2):423-40.

37. Yang X, Liu D, Lv N, Zhao F, Liu F, Zou J, et al. TCRklass: A New K-String–Based Algorithm for Human and Mouse TCR Repertoire Characterization. *The Journal of Immunology.* 2015;194(1):446-54.

38. Madi A, Shifrut E, Reich-Zeliger S, Gal H, Best K, Ndifon W, et al. T-cell receptor repertoires share a restricted set of public and abundant CDR3 sequences that are associated with self-related immunity. *Genome Res.* 2014;24(10):1603-12.

39. Madi A, Poran A, Shifrut E, Reich-Zeliger S, Greenstein E, Zaretsky I, et al. T cell receptor repertoires of mice and humans are clustered in similarity networks around conserved public CDR3 sequences. *Elife.* 2017;6.

40. Holder A, Mirczuk SM, Fowkes RC, Palmer DB, Aspinall R, and Catchpole B. Perturbation of the T cell receptor repertoire occurs with increasing age in dogs. *Developmental and Comparative Immunology.* 2018;79:150-7.

41. Contento RL, Molon B, Boularan C, Pozzan T, Manes S, Marullo S, et al. CXCR4-CCR5: A couple modulating T cell functions. *Proceedings of the National Academy of Sciences.* 2008;105(29):10101-6.

42. Chong SZ, Evrard M, Goh CC, and Ng LG. Illuminating the covert mission of mononuclear phagocytes in their regional niches. *Current Opinion in Immunology.* 2018;50:94-101.

43. Caron G, Le Gallou S, Lamy T, Tarte K, and Fest T. CXCR4 Expression Functionally Discriminates Centroblasts versus Centrocytes within Human Germinal Center B Cells. *The Journal of Immunology.* 2009;182(12):7595-602.

44. Abbott JD, Huang Y, Liu D, Hickey R, Krause DS, and Giordano FJ. Stromal cell-derived factor-1α plays a critical role in stem cell recruitment to the heart after myocardial

infarction but is not sufficient to induce homing in the absence of injury. *Circulation.* 2004;110(21):3300-5.

45. Heinze B, Fuss CT, Mulatero P, Beuschlein F, Reincke M, Mustafa M, et al. Targeting CXCR4 (CXC Chemokine Receptor Type 4) for Molecular Imaging of Aldosterone-Producing Adenoma. *Hypertension.* 2018;71(2):317-25.

46. Ertl G, and Frantz S. Wound model of myocardial infarction. *American Journal of Physiology-Heart and Circulatory Physiology.* 2005;288(3):H981-H3.

47. Yan X, Anzai A, Katsumata Y, Matsuhashi T, Ito K, Endo J, et al. Temporal dynamics of cardiac immune cell accumulation following acute myocardial infarction. *J Mol Cell Cardiol.* 2013;62:24-35.

48. Epelman S, Liu PP, and Mann DL. Role of Innate and Adaptive Immunity in Cardiac Injury and Repair Slava. *Nature review immunology.* 2015;15(2):117-29.

49. Latet SC, Hoymans VY, Van Herck PL, and Vrints CJ. The cellular immune system in the post-myocardial infarction repair process. *International Journal of Cardiology.* 2015;179:240-7.

50. Prabhu SD, and Frangogiannis NG. The Biological Basis for Cardiac Repair After Myocardial Infarction: From Inflammation to Fibrosis. *Circ Res.* 2016;119(1):91-112.

51. Van der Borght K, and Lambrecht BN. Heart macrophages and dendritic cells in sickness and in health: A tale of a complicated marriage. *Cellular Immunology.* 2018.

52. Nahrendorf M, Pittet MJ, and Swirski FK. Monocytes: protagonists of infarct inflammation and repair after myocardial infarction. *Circulation.* 2010;121(22):2437-45.

53. Frantz S, Hofmann U, Fraccarollo D, Schäfer A, Kranepuhl S, Hagedorn I, et al. Monocytes/macrophages prevent healing defects and left ventricular thrombus formation after myocardial infarction. *FASEB Journal.* 2013;27(3):871-81.

54. Mathes D, Weirather J, Nordbeck P, Arias-Loza AP, Burkard M, Pachel C, et al. CD4+FOXP3+T-cells contribute to myocardial ischemia-reperfusion injury. *Journal of Molecular and Cellular Cardiology.* 2016;101:99-105.

55. Wang YP, Xie Y, Ma H, Su SA, Wang YD, Wang JA, et al. Regulatory T lymphocytes in myocardial infarction: A promising new therapeutic target. *Int J Cardiol.* 2016;203:923-8.

56. Xiu J, Cui K, Wang Y, Zheng H, Chen G, Feng Q, et al. Prognostic Value of Myocardial Perfusion Analysis in Patients with Coronary Artery Disease: A Meta-Analysis. *Journal of the American Society of Echocardiography.* 2017;30(3):270-81.

57. Kallikourdis M. T cell responses to tumor: how dominant assumptions on immune activity led to a neglect of pathological functions, and how evolutionary considerations can help identify testable hypotheses for improving immunotherapy. *Cancer Immunology, Immunotherapy.* 2018;0(0):1-10.

58. Hu M, Watson D, Zhang GY, Graf N, Wang YM, Sartor M, et al. Long-term cardiac allograft survival across an MHC mismatch after "pruning" of alloreactive CD4 T cells. *Journal of immunology (Baltimore, Md : 1950).* 2008;180(10):6593-603.

59. Klingenberg R, Brokopp CE, Grives A, Courtier A, Jaguszewski M, Pasqual N, et al. Clonal restriction and predominance of regulatory T cells in coronary thrombi of patients with acute coronary syndromes. *Eur Heart J.* 2015;36(17):1041-8.

60. Heidecker B, Kittleson MM, Kasper EK, Wittstein IS, Champion HC, Russell SD, et al. Transcriptomic biomarkers for the accurate diagnosis of myocarditis. *Circulation.* 2011;123(11):1174-84.

61. Blohm JH, Blohm N, Hummel M, Muller HH, Rohde M, Hetzer R, et al. Detection of clonal T-cell-receptor (TCR) Vbeta rearrangements in explanted dilated cardiomyopathy

hearts by semi-nested PCR, GeneScan, and direct sequencing. *Med Sci Monit Basic Res.* 2013;19:111-7.

62. Lindskog C, Linne J, Fagerberg L, Hallstrom BM, Sundberg CJ, Lindholm M, et al. The human cardiac and skeletal muscle proteomes defined by transcriptomics and antibody-based profiling. *BMC Genomics.* 2015;16:475.

63. Lv H, and Lipes MA. Role of Impaired Central Tolerance to α-Myosin in Inflammatory Heart Disease. *Trends in Cardiovascular Medicine.* 2012;22(5):113-7.

64. Murphy KM. *Janeway's Immunobiology.* Taylor & Francis Group; 2011.

65. Wang Y, Dembowsky K, Chevalier E, Stuve P, Korf-Klingebiel M, Lochner M, et al. C-X-C Motif Chemokine Receptor 4 Blockade Promotes Tissue Repair After Myocardial Infarction by Enhancing Regulatory T Cell Mobilization and Immune-Regulatory Function. *Circulation.* 2019;139(15):1798-812.

66. Battaglia A, Ferrandina G, Buzzonetti A, Malinconico P, Legge F, Salutari V, et al. Lymphocyte populations in human lymph nodes. Alterations in CD4+ CD25+ T regulatory cell phenotype and T-cell receptor Vbeta repertoire. *Immunology.* 2003;110(3):304-12.

67. Ertl G, and Frantz S. Healing after myocardial infarction. *Cardiovasc Res.* 2005;66(1):22-32.

68. van der Laan AM, Ter Horst EN, Delewi R, Begieneman MP, Krijnen PA, Hirsch A, et al. Monocyte subset accumulation in the human heart following acute myocardial infarction and the role of the spleen as monocyte reservoir. *Eur Heart J.* 2014;35(6):376-85.

69 Reiter T, Kircher M, Schirbel A, Werner RA, Kropf S, Ertl G, et al. Imaging of C-X-C Motif Chemokine Receptor CXCR4 Expression After Myocardial Infarction With

[(68)Ga]Pentixafor-PET/CT in Correlation With Cardiac MRI. *JACC Cardiovasc Imaging.* 2018;11(10):1541-3.

70 Joint Working Group on Veterinary C, Voipio HM, Baneux P, Gomez de Segura IA, Hau J, and Wolfensohn S. Guidelines for the veterinary care of laboratory animals: report of the FELASA/ECLAM/ESLAV Joint Working Group on Veterinary Care. *Lab Anim.* 2008;42(1):1-11.

71 Guillen J. FELASA Guidelines and Recommendations. *Journal of the American Association for Laboratory Animal Science.* 2012;51(3):311-21.

Figures

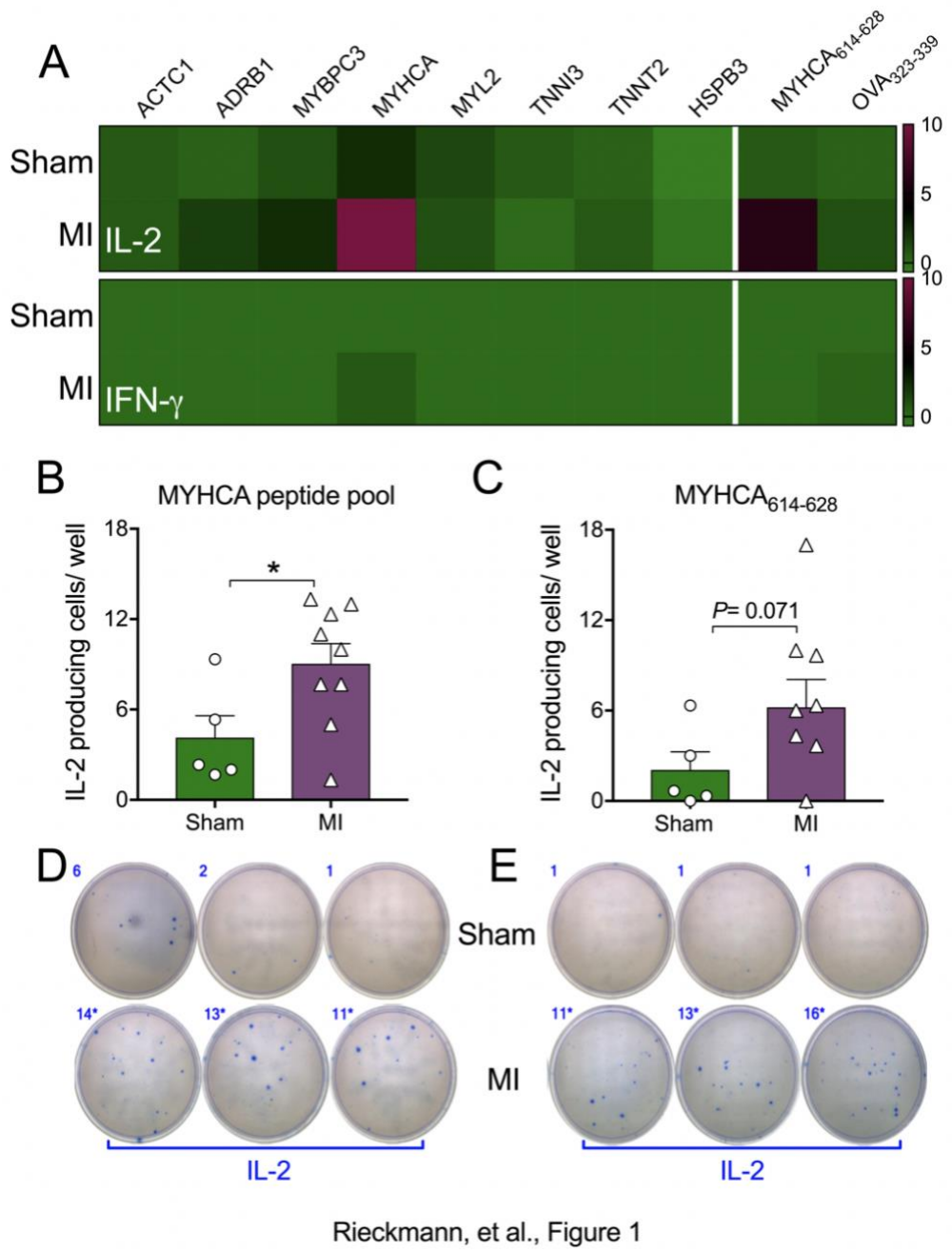

Figure 1. Cardiac epitope mapping. (**A**) Heatmaps depicting the number of specific T cell responses to defined antigens of interest. Splenocytes purified from MI or sham-operated mice (d7) were cultured in the presence of peptide pools (15 mers, MHC-II-restricted) covering the most important heart-enriched proteins, and the production of IL-2 and IFN-γ was monitored by ELISPOT as a readout for antigen-specific stimulation. ACTC1: alpha actin, cardiac muscle 1; ADRB1: adrenergic receptor beta 1; MYBPC3: myosin-ending protein C3; MYHCA: myosin

heavy chain alpha; MYL2: myosin light chain 2; TNNI3: troponin I3, cardiac muscle; TNNT2: troponin T2, cardiac muscle; HSPB3: heat shock protein family member 3. The single peptides $MYHCA_{614-628}$ (included in the MYHCA pool) and $OVA_{323-339}$ (irrelevant antigen, not expressed in the heart) were also tested. Quantification of IL-2 producing cells per well in response to MYHCA peptide pool and to $MYHCA_{614-628}$ are shown in **B** and **C**, respectively. Representative ELISPOT images of these antigens are shown in **D-E**. The bar graphs display the group mean values, the standard errors of the mean (SEMs), and the distributions of each individual value. Statistical analysis in B-C: two-tailed unpaired t-test. The symbol * indicates $P<0.05$. The data were acquired from three independent sessions.

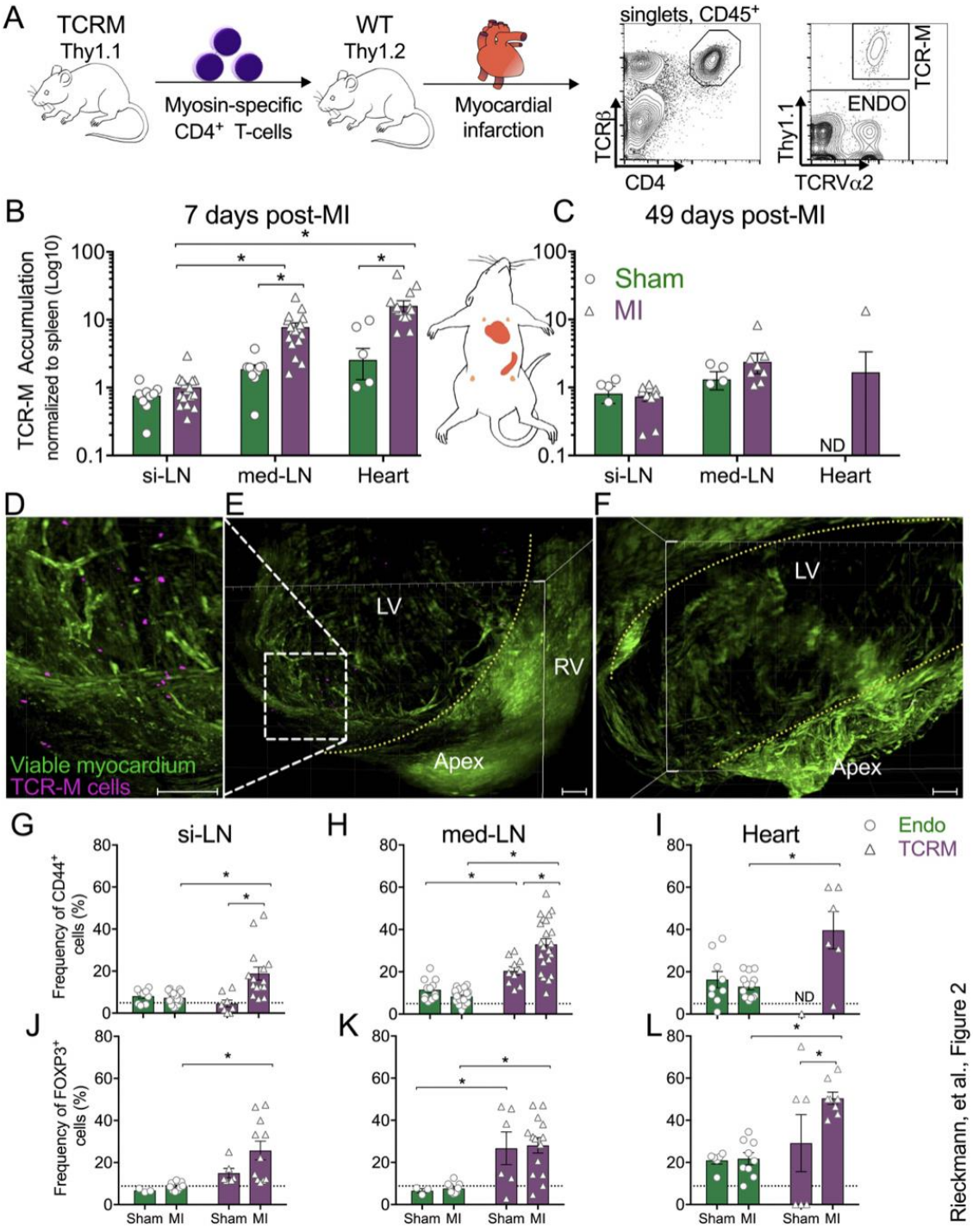

Figure 2. TCR-M cells selectively accumulate in the infarcted heart. (**A**) Experimental design and gating strategy. Thy1.1 TCR-M cells were transferred into Thy1.2 WT recipients prior to MI or sham operations. The contour plots are representative of the med-LNs 7 days after MI. The frequencies of TCR-M cells found in the subiliac LNs (si-LNs), mediastinal LNs (med-LNs,

heart-draining), and heart were assessed at days 7 (**B**) and 49 (**C**) post-MI. The accumulation index refers to the spleen-normalized frequencies. (**D-F**) Three-dimensional reconstruction of infarcted hearts (5x magnification) at days 7 **(D, E**) and 49 (**F**) post-MI. The morphological information was obtained from the autofluorescence levels acquired in the green channel. The viable myocardium appears in bright green, whereas the necrotic myocardium appears in dark green. Scale bar: 300 µm. TCR-M cells (Thy1.1^{+}) appear in magenta, and the yellow dotted lines indicate the infarct borders. (**G-L**) Frequency of CD44^{+} cells (**G-I**) and FOXP3^{+} cells (**J-L**) in the ENDO and TCR-M compartments harvested from different sites at day 7 post-MI. The dotted lines indicate the baseline frequencies (pretransfer) of CD44^{+} and FOXP3^{+} among TCR-M cells. The graphs display the group mean values (bars), the standard errors of the mean (SEMs), and the distributions of each individual value. (**B-C**) The green and magenta gridded bars represent sham- and MI-operated mice, respectively. (**G-L**) The green and magenta gridded bars represent endogenous CD4^{+} T cells and TCR-M cells, respectively. The data were acquired in at least two independent sessions; MI (n=7-23) and sham (n=3-12). Statistical analyses: two-way ANOVA followed by Sidak's multiple comparisons test. The symbol * indicates $P<0.05$.

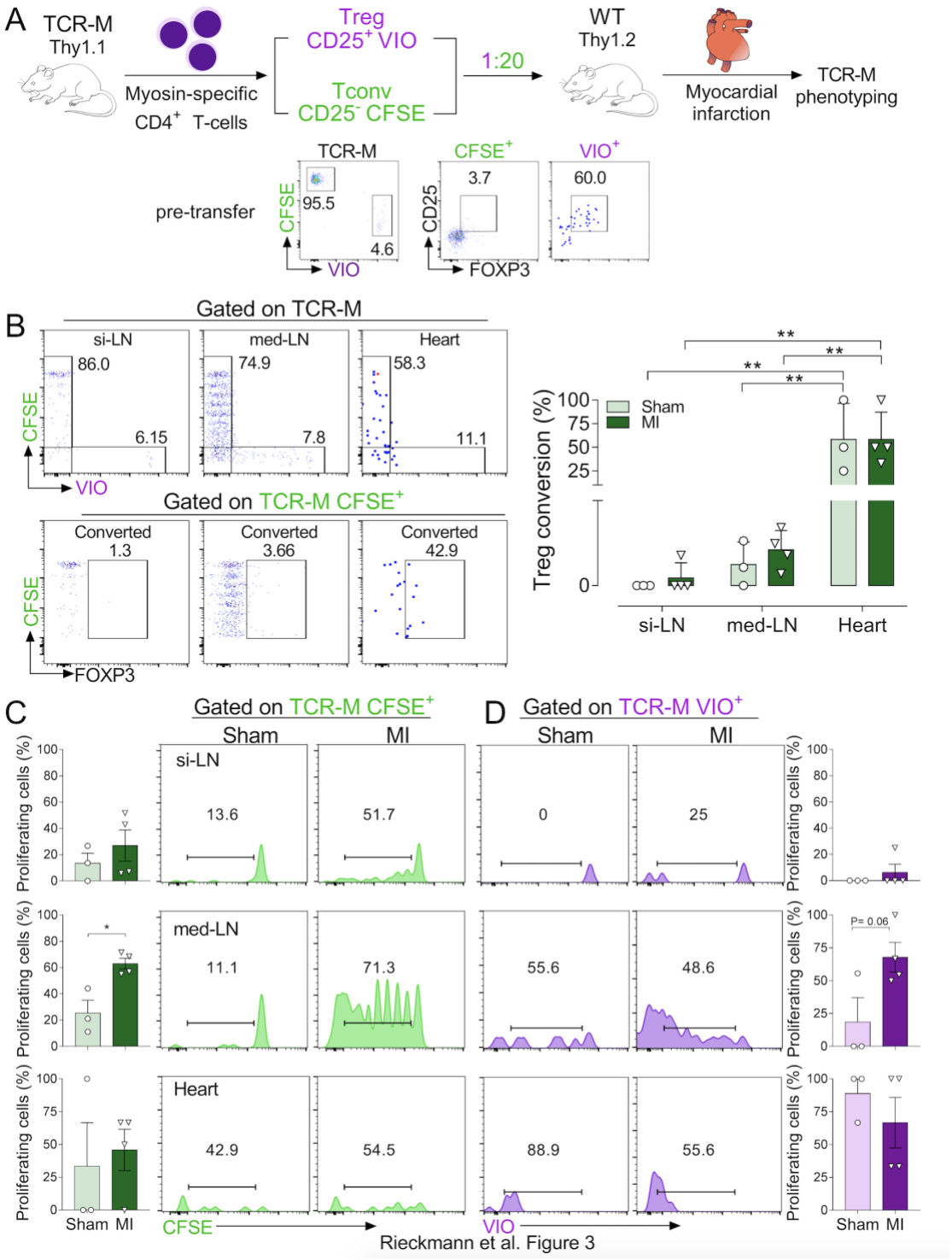

Figure 3. *In vivo* TCR-M conversion to FOXP3⁺ regulatory T cells. (**A**) Experimental design and gating strategy. Before adoptive transfer, Thy1.1⁺ TCR-M cells were enriched for Tconv (CD25⁻) and Treg (CD25⁺) cells through magnetic cell sorting and labeled with distinct, subset-

specific cell tracer dyes (CFSE and VIO, respectively). Treg and Tconv TCR-M populations were mixed in a 1:20 ratio (resembling the physiological condition) and then transferred into Thy1.2 WT recipients one day prior to MI or sham operations. The flow cytometry plots depict the pretransfer levels of FOXP3 in each compartment. (**B**) Analysis of Treg conversion from TCR-M cells in the subiliac (si-LN), mediastinal (med-LN) and heart tissues of mice 5 days after MI. "Converted Tregs" were defined as $Thy1.1^{+}CFSE^{+}$ cells that acquired FOXP3 expression after MI, as the $CFSE^{+}$ cells were $FOXP3^{-}$ prior to cell transfer. **Panels C, D**: The proliferation of conventional TCR-M cells ($Thy1.1^{+}CFSE^{+}FOXP3^{-}$) and T regulatory TCR-M cells ($Thy1.1^{+}VIO^{+}FOXP3^{+}$) was assessed through the dilution of CFSE and VIO dyes, respectively. The bar graphs display group mean values (bars), standard errors of the mean (SEMs), and distributions of each sample. Green bars represent the sham-operated group, whereas the red gridded bars represent the MI group. Statistical analysis in B: two-way ANOVA followed by Tukey's multiple comparisons test. The symbol ** indicates $P<0.01$. Statistical analysis in C and D: two-tailed unpaired T test. The symbol * indicates $P<0.05$.

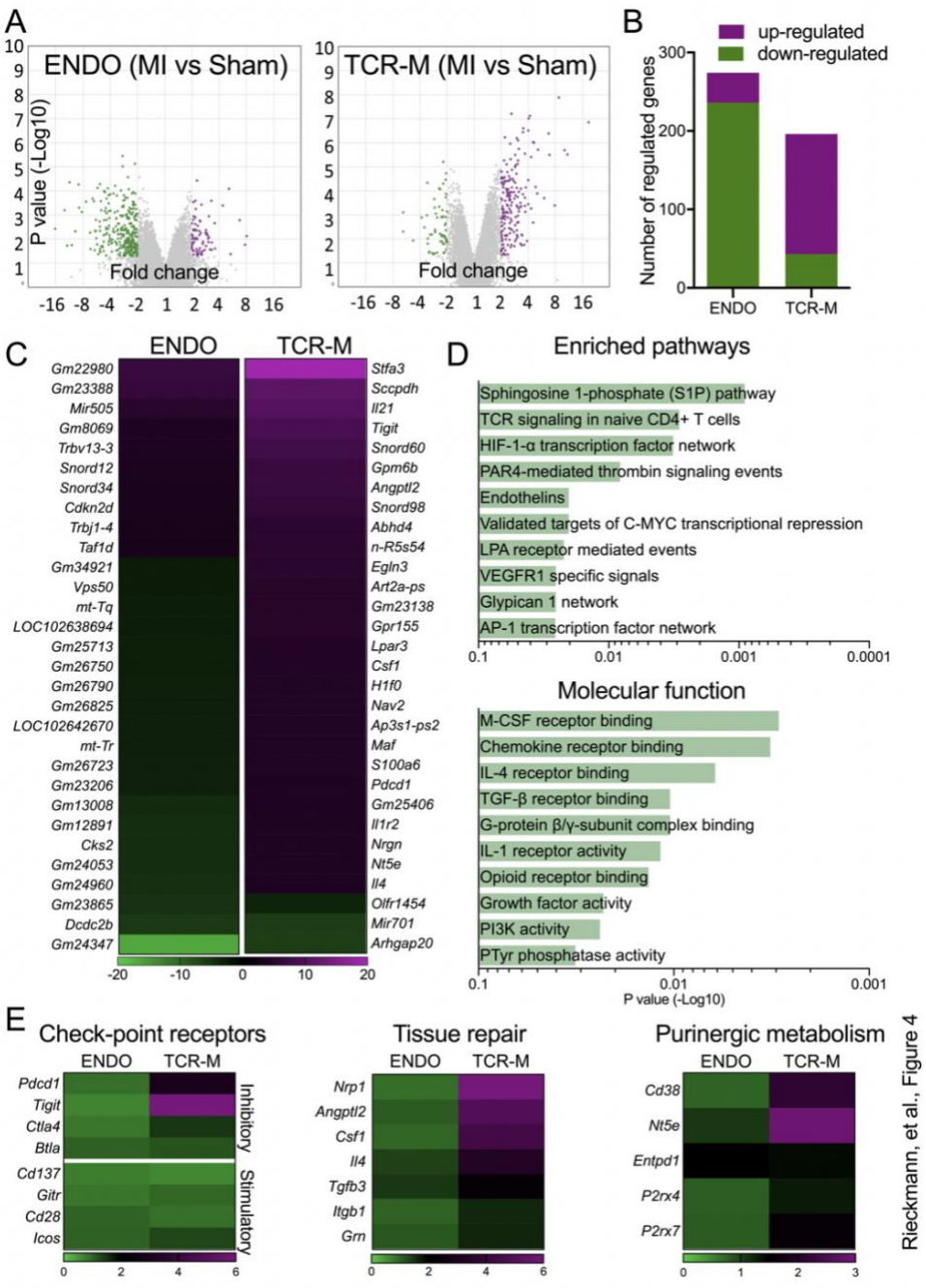

Figure 4. TCR-M cells activated in the MI context acquire a nonclassical gene expression signature enriched with pro-healing factors. Adoptively transferred TCR-M cells (defined as $CD4^+TCR\beta^+Thy1.1^+TCV\alpha2^+$ singlets) and polyclonal endogenous $CD4^+$ (ENDO, defined as $CD4^+TCR\beta^+Thy1.1^-$ singlets) were sorted from the med-LNs of MI- and sham-operated mice 7 days post-MI and used for downstream gene expression profiling. (**A**) Volcano plots comparing

the gene expression levels of ENDO and TCR-M cells post-MI/sham operation. The repressed and induced genes (±2-fold change, $P<0.05$) are highlighted in green and magenta, respectively. (**B**) Total number of up- and downregulated genes in each T cell subset. (**C**) Top 30 differentially expressed genes (MI vs sham, $P<0.05$) in each T cell subset. (**D**) Unsupervised pathway enrichment analyses and gene clustering according to molecular function (TCR-M subset). The bar lengths indicate the adjusted P values (Fisher's statistical test). (**E**) Normalized relative expression levels (MI: sham) of specific gene sets related to T cell activation (checkpoint receptors), tissue repair and purinergic metabolism. The color scale represents the normalized gene expression levels (MI vs sham) in ENDO and TCR-M cells. MI (n=5) and sham (n=3) from one session.

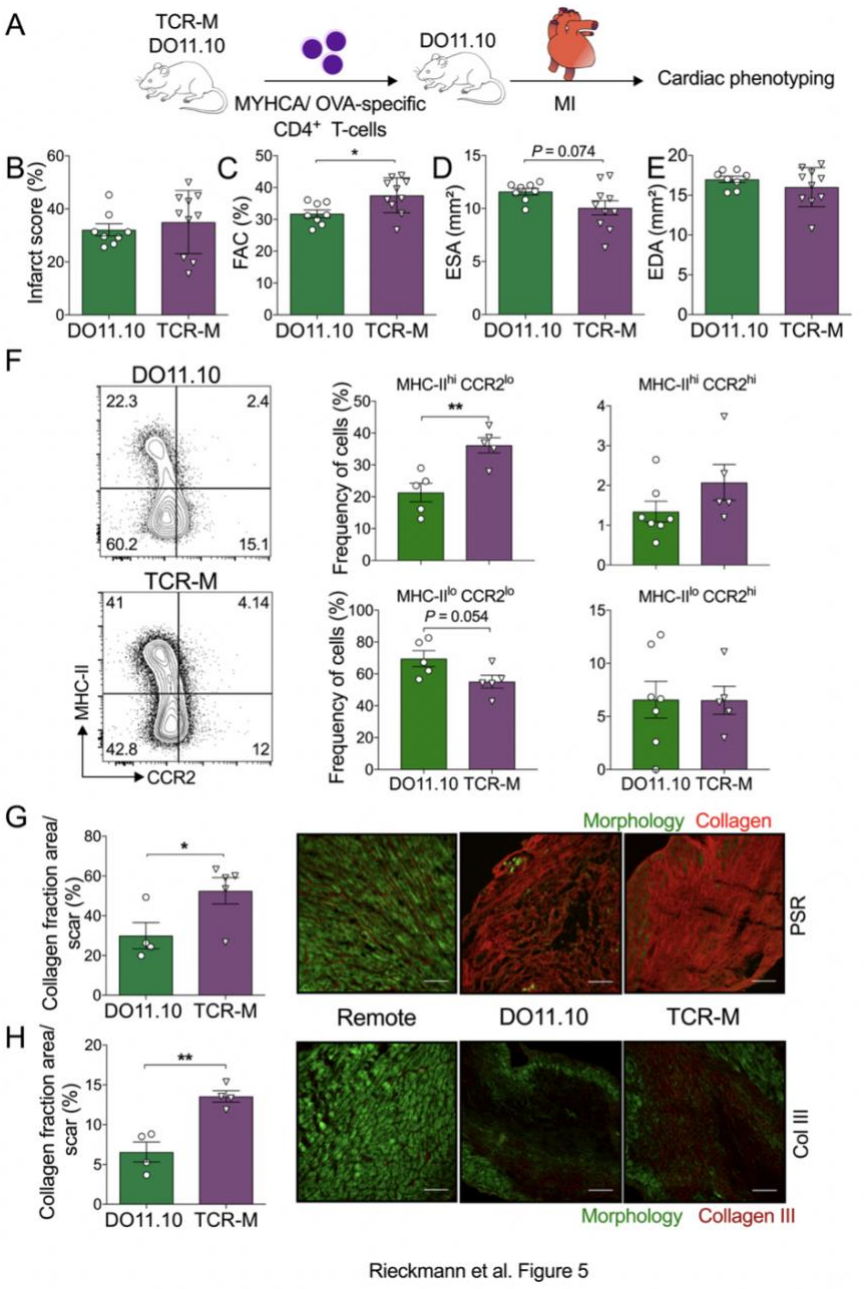

Figure 5. Heart-specific CD4⁺ T cells activated in the MI context exert cardioprotective effects. (**A**) Experimental design: TCR-M cells (specific for the cardiac antigen $MYCA_{614-629}$) and DO11.10 cells (specific for the irrelevant antigen $OVA_{323-339}$) were adoptively transferred into DO11.10 mice prior to MI or sham operation, and the cardiac outcomes were monitored at the peak of the healing phase (day 7). (**B**) The infarct size and long parasternal axis (apex-aortic valve) were assessed by echocardiography. The fractional area change (FAC, **C**), end-systolic

area (EFA, **D**), and end-diastolic area (EDA, **E**) at the mid-papillary level were assessed by echocardiography. (**F**) Cardiac macrophages, defined as $CD45^{+}CD11b^{+}Ly6G^{-}CD64^{+}$ singlets, were stratified into four major subsets according to CCR2 and MHC-II expression, and the effects of DO11.10 vs TCR-M cells on each subset's distribution were assessed (day 5). (**G**) The collagen area in scar tissue at 5 days post-MI in DO11.10- and TCR-M-transferred mice was quantified by Picrosirius Red staining (PSR). (**H**) Immunofluorescence of collagen III and its quantification in scar tissue 5 days post-MI in DO11.10 and TCR-M-transferred mice. Scale bar: 100 µM. The bar graphs display the group mean values (bars), the standard errors of the mean (SEMs) and the distributions of each individual sample. Statistical analysis: two-tailed unpaired t-test. The symbols * and ** indicate $P<0.05$ and $P<0.01$, respectively. The data from TCR-M recipients (n=5-10) and DO11.10 recipients (7-9) were acquired in three sessions.

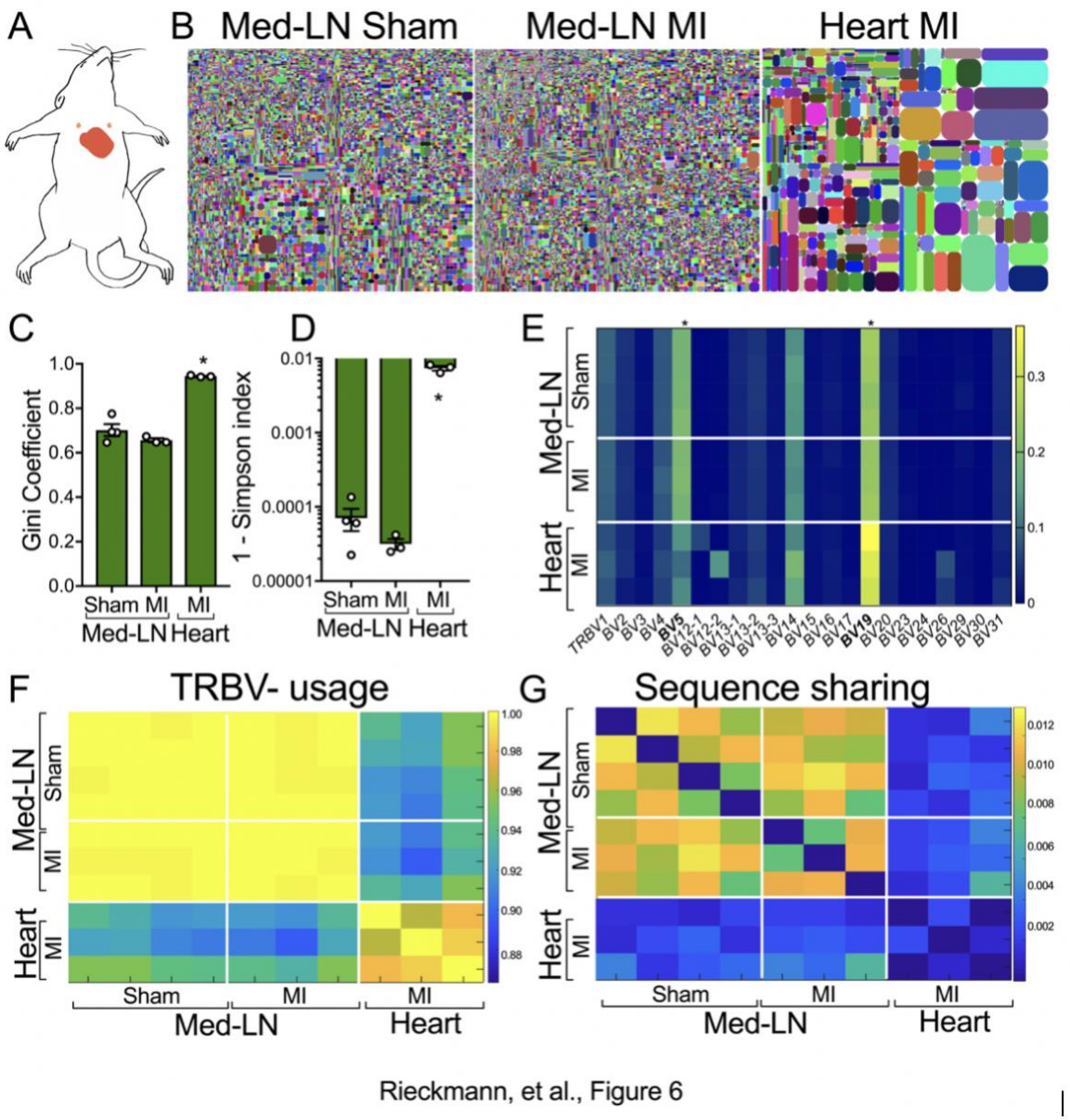

Figure 6. CD4$^+$ T cells infiltrating the murine infarcted myocardium are clonally expanded and exhibit a unique repertoire signature. (**A**) T helper cells were purified by FACS from the heart and med-LNs of MI- and sham-operated mice (day 7). (**B**) Tree maps of representative repertoires from each group. Each spot represents a unique TRBV CDR3 recombination, and the size of each spot denotes its relative frequency. The unevenness of the spots indicates clonal expansions. (**C**) The repertoire evenness was assessed by the Gini coefficient. (**D**) The repertoire

diversity was assessed based on 1-Simpson's diversity index. (**E**) Heat map depicting the TRBV gene usage in each group. The symbol * at the top of the graph indicates a statistically significant difference ($P<0.05$) between the cardiac and LN repertoires, as determined by two-way ANOVA followed by Tukey's multiple comparisons test. (**F**) Correlation among the frequencies of the TRBV gene segment between any two given samples. (**G**) Heat map showing the degree of TRBV CDR3 sequence sharing (Jaccard index) between any two given samples. The bar graphs in C-D display the group mean values (bars), the standard errors of the mean (SEMs) of three to four samples per group, and the distributions of each individual value. Statistical analyses: one-way ANOVA followed by Dunnett's multiple comparisons test. The symbol * indicates $P<0.05$ compared with all the other groups.

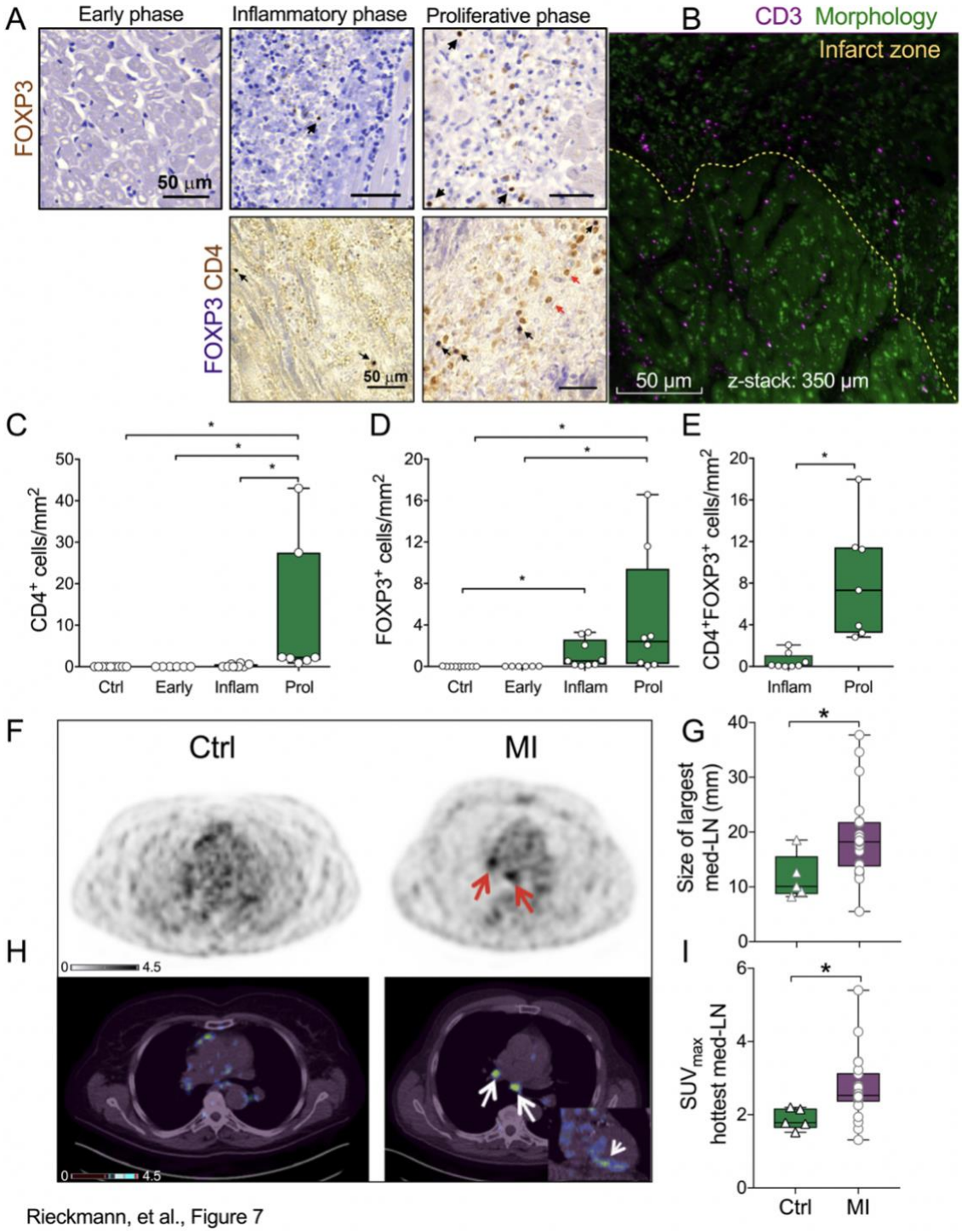

Rieckmann, et al., Figure 7

Figure 7. A heart/T cell axis in MI patients. (A-E) Histological analyses of cardiac autopsies revealed that T helper cells also accumulate in the human infarcted myocardium, particularly during the proliferative (wound healing) phase. (**A**) Representative IHC micrographs showing the

presence of $FOXP3^+$ (black arrow) and $CD4^+$ (red arrow) cells in cardiac tissues. (**B**) Light-sheet microscopy depicting the presence of $CD3^+$ T cells in the infarcted human myocardium. Scale bar 50 µm, z-stack: 350 µm (**C-E**) Numbers of $CD4^+$, $FOXP3^+$ and $CD4^+$ $FOXP3^+$ cells/mm^2 in each phase after MI (Inflam: Inflammatory phase; prol: proliferative phase). The whiskers represent the percentile range with the medians ± confidence intervals from six to nine samples per group. Nonparametric statistical test: Kruskal-Wallis corrected for multiple comparisons using Dunn's test. The symbol * indicates $P<0.05$. (**F-H**) Transaxial slices of positron emission tomography (PET; (**F**)) and fused PET/computed tomography (PET/CT, (**H**)) showing increased CXCR4 expression in med-LNs after MI (arrows) and in the infarcted myocardium (insert). Both the med-LN sizes (**G**) and CXCR4 expression (as assessed by standardized uptake values (SUV; (**I**)) were found to be increased after MI. The data are presented as box plots showing the medians, 25^{th}-75^{th} percentiles (boxes) and 5^{th}-95^{th} percentiles (whiskers) of six to nine cardiac autopsies, or 26 patients (PET-CT) per group. Statistical analyses: Fisher's exact test (**C-E**) and t-/Welch-test (**G, I**); the symbol * indicates $P<0.05$.